Journal of Solid Mechanics Vol. 7, No. 2 (2015) pp. 204-222

Application of Case I and Case II of Hill's 1979 Yield Criterion to Predict FLD

M. Aghaie-Khafri *, M. Torabi-Noori

Faculty of Mechanical Engineering, K.N. Toosi University of Technology, Postal Code: 1999143344, Tehran, Iran

Received 8 March 2015; accepted 6 May 2015

ABSTRACT

Forming limit diagrams (FLDs) are calculated based on both the Marciniak and Kuczynski (M-K) model and the analysis proposed by Jones and Gillis (J-G). J-G analysis consisted of plastic deformation approximation by three deformation phases. These phases consisted of homogeneous deformation up to the maximum load (Phase I), deformation localization under constant load (phase II) and local necking with a precipitous drop in load (phase III). In the present study, case I and case II of Hill's non-quadratic yield function were used for the first time. It is assumed that sheets obey the power-law flow rule and in-plane isotropy is satisfied. Calculated FLDs from this analysis are compared with the experimental data of aluminum alloys 3003-O, 2036-T4 and AK steel reported by other references. Calculated FLDs showed that limit strain predictions based on case I and case II of the Hill's non-quadratic yield function are fairly well correlated to experiments when J-G model is used.

Keywords : Yield function; Forming limit diagrams; Localization.

1 INTRODUCTION

IN sheet metal, forming useful deformation is limited by the occurrence of plastic instability and necking. Forming limit diagram (FLD) , was introduced by Keeler [1] and Goodwin [2], shows the relationship between minor and major principal strains under diffuse or localized necking in a plane-stress condition. Experimental FLDs were developed for a wide range of sheet metals and sandwich sheets [3,4]. However, experimental determination of the FLDs is associated with practical difficulties [5]. Thus, different analytical and numerical models have been developed to predict limit strains and to construct FLD [6,7]. These models are mostly on the basis of different yield and instability criteria and flow or hardening rules.

Hart [8] developed a general analysis of plastic instability of tension test with special attention to the influence of strain-rate-sensitivity (SRS) of the flow stress. Hill described the localized necking in thin sheets under plane stress states [9]. However, Hill's theory does not take into account the SRS of the material. Jones and Gillis [10] model was based on Hart's approach. Their criterion for plastic instability is taken as the formation of a severe localization of the deformation such as a neck.

Marciniak and Kuczynski (M-K) [11] approach is usually considered to model FLDs [12]. This approach consisted of the assumption of an initial imperfection in the sheet material in the form of a line of slightly reduced thickness, or groove, across the test specimen. A different approach was introduced by the Jones-Gillis (J-G) theory

* Corresponding author. Tel.: +98 9123088389; Fax: +98 21 88674748.
E-mail address: maghaei@kntu.ac.ir (M. Aghaei-Khafri).

[13]. They developed a model that eliminates the necessity for the determination of the initial heterogeneity coefficient.

The capability of J-G analysis to predict FLDs have been discussed by a number of studies. Choi et al [14,15] and Jones and Gillis [16,17], applied J-G model using a generalized anisotropic yield criterion for determination of FLDs. Pishbin and Gillis [18] developed J-G model by application of case IV of non-quadratic Hill's yield criterion. Aghaie-Khafri and Mahmudi [19,20] improved J-G model by application of Hosford's yield criterion for the prediction of the FLDs for aluminum alloys sheets. Noori and Mahmudi [21] used J-G model to predict FLDs using three different yield criteria. More recently, Rezaee-Bazzaz et al [22] used Hill's 1993 criterion and J-G model for predicting FLDs.

Some other recent investigations on the FLD calculation are as follows. The validation of the deformation path insensitive formulae of the forming limit criterion and the validation of forming condition independence of the forming limit criterion to justify its feature as a material property for typical room temperature thin sheet forming under the plane stress condition was presented by Chung et al [23]. Avila and Vieira studied the M-K model based on five different yield criteria [24].The FLD of a half-hard aluminium alloy (AA1100-H24) sheet was obtained theoretically for linear strain paths using two different approaches: phenomenological theory and crystal plasticity theory by Chiba et al [25]. Panich et al investigated experimentally determined and theoretically calculated FLDs and FLSDs of two AHS steels, DP780 and TRIP780 steel. The FLDs and FLSDs based on experimental data were compared with the FLDs and FLSDs based on the M–K model [26]. The M–K model with the linear and nonlinear deformation paths has been studied by Assempour et al [27]. The onset of localized necking in anisotropic metal sheets was analyzed by Kuroda et al [28]. Four different anisotropic plasticity models were used. For all four models, the yield surfaces and hardening behavior are fitted to agree with experimental results of a cold-rolled steel sheet.

In the present work, for the first time case I and case II of Hill's 1979 criterion in conjunction with the J-G analysis and M-K model is used to predict FLDs. The results of calculation were compared to experiments.

2 ANALYSIS

2.1 Yield criteria

In this study, case I and case II of Hill's non-quadratic criterion were used in order to calculate the stress components from the strain and strain rate components. Hill proposed the following anisotropic yield criterion:

$$f\left|\sigma_2-\sigma_3\right|^M+g\left|\sigma_3-\sigma_1\right|^M+h\left|\sigma_1-\sigma_2\right|^M+a\left|2\sigma_1-\sigma_2-\sigma_3\right|^M+b\left|2\sigma_2-\sigma_3-\sigma_1\right|^M \\ +c\left|2\sigma_3-\sigma_1-\sigma_2\right|^M=\bar{\sigma}^M \tag{1}$$

For $a=h=b=0$ and $f=g$ (case 1):

$$c\left|\sigma_1+\sigma_2\right|^M+f\left(\left|\sigma_1\right|^M+\left|\sigma_2\right|^M\right)=\bar{\sigma}^M \tag{2}$$

and for $a=b, f=g=c=0$ (case II)

$$a(\left|2\sigma_1-\sigma_2\right|^M+\left|2\sigma_2-\sigma_1\right|^M)+h\left|\sigma_1-\sigma_2\right|^M=\bar{\sigma}^M \tag{3}$$

where *M* is considered as a flexible index for comparing with experiments. Considering the following equation that is given by Hill [29]:

$$R=\frac{\left(2^{M-1}+2\right)a-c+h}{\left(2^{M-1}-1\right)a+2c+f} \tag{4}$$

and uniaxial tension condition, $\sigma_e=\sigma_1$, the more common form of case I and case II of Hill's criterion can be obtained as:

Case I:

$$(2R+1)\left(\left|\sigma_1\right|^M+\left|\sigma_2\right|^M\right)-R\left|\sigma_1+\sigma_2\right|^M=(R+1)\bar{\sigma}^M \tag{5}$$

Case II:

$$\left|2\sigma_1-\sigma_2\right|^M+\left|2\sigma_2-\sigma_1\right|^M+((R-1)(2^{M-1}-1)-3)\left|\sigma_1-\sigma_2\right|^M=(R+1)(2^{M-1}-1)\bar{\sigma}^M \tag{6}$$

where σ_1 and σ_2 are the principal stress components in the sheet plane and R is the plastic anisotropy ratio.

Based on the case I of Hill's yield criterion, the equivalent strain rate is given by [30]:

$$\dot{\bar{\varepsilon}}=(c_1g_1+c_2g_2)^{(M-1)/M} \tag{7}$$

where g_1 and g_2 are defined as following:

$$g_1=\left|\dot{\varepsilon}_1\right|^{M/(M-1)}+\left|\dot{\varepsilon}_2\right|^{M/(M-1)} \tag{8}$$

$$g_2=\left|\dot{\varepsilon}_1-\dot{\varepsilon}_2\right|^{M/(M-1)} \tag{9}$$

For case II we have:

$$g_1=\left|2\dot{\varepsilon}_1+\dot{\varepsilon}_2\right|^{M/(M-1)}+\left|2\dot{\varepsilon}_2+\dot{\varepsilon}_1\right|^{M/(M-1)} \tag{10}$$

$$g_2=\left|\dot{\varepsilon}_1+\dot{\varepsilon}_2\right|^{M/(M-1)} \tag{11}$$

c_1 and c_2 can be determined based on the principal of the work equivalence.

In the balanced biaxial tension, $\sigma_1=\sigma_2$ and $c_1=c_2$. Concerning these conditions and equivalent stress and strain equations:

For case I:

$$c_1=\left[\frac{R+1}{2R+1-2^{M-1}R}\right]^{1/(M-1)} \tag{12}$$

For case II:

$$c_1=\left[\frac{(R+1)\left(2^{M-1}-1\right)}{3^M+2^{M-1}\left((R-1)\left(2^{M-1}-1\right)-3\right)}\right]^{1/M} \tag{13}$$

For the shear deformation condition, we have $\sigma_1=\sigma_2$ and $c_1=c_2$. Thus,

For case I:

$$c_2=\left[\frac{R+1}{2(2R+1)}\right]^{1/(M-1)}\left[1-\left(\frac{2R+1}{2R+1-2^{M-1}R}\right)^{1/(M-1)}\right] \tag{14}$$

For case II:

$$c_2 = \left[\frac{(R+1)\left(2^{M-1}-1\right)}{2}\right]^{1/M-1} - \left(\frac{3^M}{2}\right)^{1/M-1} c_3 \tag{15}$$

Finally, more simplified form of the equivalent strain rate can be drawn as:
For case I:

$$\dot{\bar{\varepsilon}} = \left[\begin{array}{l}\left(\frac{R+1}{2R+1-2^{M-1}R}\right)^{1/(M-1)}\left(\left|\dot{\varepsilon}_1\right|^{M/(M-1)} + \left|\dot{\varepsilon}_2\right|^{M/(M-1)}\right) + \\ \left(\frac{R+1}{2(2R+1)}\right)^{1/(M-1)}\left(1-\left(\frac{2R+1}{2R+1-2^{M-1}R}\right)^{1/(M-1)}\right)\left|\dot{\varepsilon}_1-\dot{\varepsilon}_2\right|^{M/(M-1)}\end{array}\right]^{(M-1)/M} \tag{16}$$

For Case II:

$$\dot{\bar{\varepsilon}} = \left(z_1\left(\left|2\dot{\varepsilon}_1+\dot{\varepsilon}_2\right|^{M/(M-1)} + \left|2\dot{\varepsilon}_2+\dot{\varepsilon}_1\right|^{M/(M-1)}\right) + z_2\left|\dot{\varepsilon}_1+\dot{\varepsilon}_2\right|^{M/(M-1)}\right)^{(M-1)/M} \tag{17}$$

where,

$$z_1 = \left((R+1)(2^{M-1}-1)/\left(3^M + 2^{M-1}\left((R-1)(2^{M-1}-1)-3\right)\right)\right)^{1/M}$$
$$z_2 = \left((R+1)(2^{M-1}-1)/2\right)^{1/(M-1)} - 2\left(3/2\right)^{M/(M-1)} z_1$$

Principal stresses σ_1 and σ_2 can be calculated as:

$$\sigma_1 = b_1\bar{\sigma} \tag{18}$$

where b_1 is a constant that is defined as:
For case I:

$$b_1 = \left(\frac{R+1}{(2R+1)\left(1+\gamma^M\right) - R(1+\gamma)^M}\right)^{(1/M)} \tag{19}$$

For case II:

$$b_1 = \left[\frac{(R+1)\left(2^{M-1}-1\right)}{(2-\gamma)^M + (2\gamma-1)^M + \left((R-1)\left(2^{M-1}-1\right)-3\right)(1-\gamma)^M}\right]^{1/M} \tag{20}$$

and,

$$\sigma_2 = \gamma\sigma_1 \tag{21}$$

where, γ is the ratio of principal stresses.

Using associated flow rules for plastic deformation, when the stress or the stress ratio is known, the corresponding strain can be found from the following relationships:

For case I:

$$\dot{\varepsilon}_1 = \dot{\lambda}\left[\left(2R+1\right)\sigma_1^{M-1} - R\left(\sigma_1+\sigma_2\right)^{M-1}\right] \tag{22}$$

$$\dot{\varepsilon}_2 = \dot{\lambda}\left[\left(2R+1\right)\sigma_2^{M-1} - R\left(\sigma_1+\sigma_2\right)^{M-1}\right] \tag{23}$$

where,

$$\dot{\lambda} = \frac{\dot{\bar{\varepsilon}}}{(R+1)\bar{\sigma}^{M-1}}$$

For case II:

$$\dot{\varepsilon}_1 = \dot{\lambda}\left[2\left(2\sigma_1-\sigma_2\right)^{M-1} - \left(2\sigma_2-\sigma_1\right)^{M-1} + ((R-1)(2^{M-1}-1)-3)\left(\sigma_1-\sigma_2\right)^{M-1}\right] \tag{24}$$

$$\dot{\varepsilon}_2 = \dot{\lambda}\left[2\left(2\sigma_2-\sigma_1\right)^{M-1} - \left(2\sigma_1-\sigma_2\right)^{M-1} - ((R-1)(2^{M-1}-1)-3)\left(\sigma_1-\sigma_2\right)^{M-1}\right] \tag{25}$$

where,

$$\dot{\lambda} = \frac{\dot{\bar{\varepsilon}}}{(R-1)(2^{M-1}-1)\bar{\sigma}^{M-1}}$$

The value of ρ can be determined from Eqs. (22) and (23):

For case I:

$$\rho = \frac{\left(2R+1\right)\gamma^{M-1} - R\left(1+\gamma\right)^{M-1}}{2R+1-R\left(1+\gamma\right)^{M-1}} \tag{26}$$

For case II:

$$\rho = \frac{2\left(2\gamma-1\right)^{M-1} - \left(2-\gamma\right)^{M-1} - \left((R-1)(2^{M-1}-1)-3\right)\left(1-\gamma\right)^{M-1}}{2\left(2-\gamma\right)^{M-1} - \left(2\gamma-1\right)^{M-1} + \left((R-1)(2^{M-1}-1)-3\right)\left(1-\gamma\right)^{M-1}} \tag{27}$$

where,

$$\rho = \frac{\dot{\varepsilon}_2}{\dot{\varepsilon}_1} \tag{28}$$

2.2 J-G model

According to J-G model, plastic deformation is approximated by three deformation phases as schematically indicated in Fig. 1:

Phase (I): homogeneous deformation up to the maximum load.

Phase (II): deformation localization under constant load.

Phase (III): local necking with a precipitous drop in load.

Point *H* is the transition point between phase I and II and that between phase II and III is point *J*.

Fig. 2 shows the geometry of neck formation and the element of sheet undergoing plastic deformation. Concerning the J-G analysis, logarithmic principal strains at the minimum thickness in the deforming sheet (2a) are defined as:

$$\varepsilon_2 = Ln(w/w_0) \tag{29}$$

$$\varepsilon_3 = Ln(a/h_0) \tag{30}$$

$$\varepsilon_1 = -(\varepsilon_2 + \varepsilon_3) = Ln(h_0 w_0 / aw) \tag{31}$$

According to tensor transformation, strain-rate components in the local coordinate system are:

$$\dot{\varepsilon}_x = \dot{\varepsilon}_1 \cos^2\theta + \dot{\varepsilon}_2 \sin^2\theta \tag{32}$$

$$\dot{\varepsilon}_y = \dot{\varepsilon}_1 \sin^2\theta + \dot{\varepsilon}_2 \cos^2\theta \tag{33}$$

$$\dot{\varepsilon}_z = \dot{\varepsilon}_3 \tag{34}$$

and,

$$\dot{\gamma}/2 = (\dot{\varepsilon}_1 - \dot{\varepsilon}_2)\sin\theta\cos\theta \tag{35}$$

Fig. 2 shows the local coordinate system *x, y, z*. The *y*-axis is along the direction of neck formation; the *z*-axis coincides with the *3*-axis; and the *x*-axis is perpendicular to both *z* and *y*. It is assumed that during the initial homogeneous phase of the deformation average logarithmic strain rates in the length and width directions are constant. It is worth noting that these conditions hold throughout the deformation for the RHS of FLD. However, for the LHS of FLD, as neck formation proceeds, the width strain rate is assumed to be proportional to the rate in the length direction. Consequently, for the RHS for all three phases:

$$\frac{\dot{L}}{L} = \alpha = cons\tan t \tag{36}$$

$$\frac{\dot{w}}{w} = \beta = cons\tan t \tag{37}$$

In the LHS, Eqs. (36) and (37) can be used during phase I. During phases II and III, it is assumed that:

$$\frac{\dot{L}}{L} = \alpha \tag{38}$$

For the width direction, it is assumed that:

$$\dot{\varepsilon}_2 = \left(\frac{\beta}{\alpha}\right)\dot{\varepsilon}_1 \qquad \beta \le 0. \tag{39}$$

It is interesting to note that during the propagation of neck, both the longitudinal strain rate and the width strain rate are changed along the length direction. For a given material, α is held constant; β varies over a set of discrete cases from uniaxial tension to equibiaxial stretching. For uniaxial tension, $\rho = -R/(1+R)$; for plane strain tension, $\rho = 0$; and for equibiaxial stretching, $\rho = 1$.

2.2.1 Analysis of phase I

It is assumed that the initial phase of the deformation is relatively homogeneous. The Considére [31] criterion for the maximum load in 1 direction is:

$$\frac{\dot{\sigma}_1}{\sigma_1} = \dot{\varepsilon}_1 \tag{40}$$

when this condition is satisfied, phase I terminates (point *H*), as shown in Fig. 1. The assumption of an initial homogenous phase results in:

$$\dot{\varepsilon}_1 = \alpha \quad \varepsilon_1 = \alpha t \tag{41}$$

$$\dot{\varepsilon}_2 = \beta \quad \varepsilon_2 = \beta t \tag{42}$$

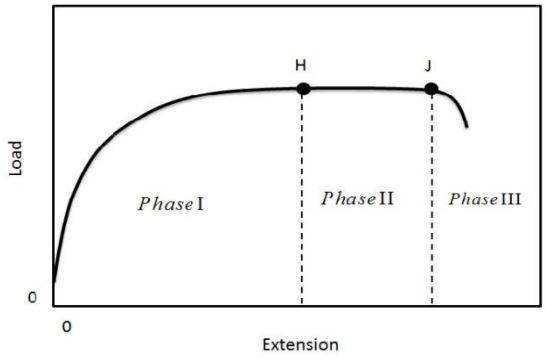

Fig.1
Schematic representation of the three deformation phases. Point *H* and *J* are, respectively, denoted as the end of homogeneous deformation (phase I) and deformation at constant load (phase II).

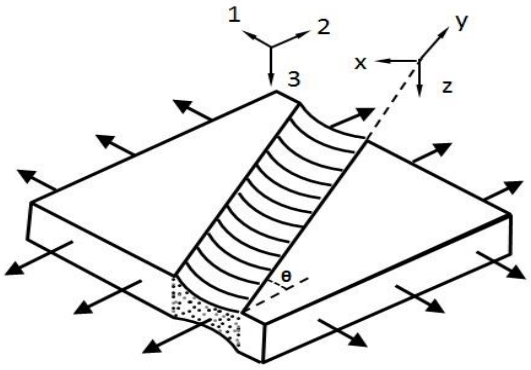

Fig.2
The geometry of neck formation in the sheet. The localized neck is inclined at an angle θ to the *2*-axis when strain rate ratio is negative.

2.2.2 Analysis of phase II

Phase II of deformation is a period of nearly constant longitudinal load and gradual concentration of the deformation into the vicinity of the critical cross-section that is straining faster near the beginning of this phase. Consequently, it is assumed that the load remains constant. It is worth noting that the assumption of homogenous deformation does not hold any more.

In the LHS of the FLD, the strain-rate ratio, is assumed to be constant. Therefore,

$$\dot{\varepsilon}_2 = \beta\dot{\varepsilon}_1 \quad \beta \le 0 \tag{43}$$

So, the stress ratio, is constant too. However, derivation of γ from ρ is not analytically achieved. From Eq. (26) and (27) we obtained:

For case I:

$$F(\gamma) = \left(2R+1\right)\gamma^{M-1} - R\left(1+\gamma\right)^{M-1} - \rho(2R+1-R\left(1+\gamma\right)^{M-1}) = 0 \tag{44}$$

For case II:

$$F(\gamma) = 2(2\gamma-1)^{M-1} - (2-\gamma)^{M-1} - q(1-\gamma)^{M-1} - \rho(2(2-\gamma)^{M-1} - (2\gamma-1)^{M-1} + q(1-\gamma)^{M-1}) \tag{45}$$

where,

$$q = \left(R-1\right)\left(2^{M-1}-1\right) - 3$$

In order to solve Eqs. (44) and (45) for γ, the numerical Newton-Raphson's method was used.

Applying energy equilibrium we have:

$$\overline{\sigma\dot{\varepsilon}} = \sigma_1\dot{\varepsilon}_1 + \sigma_2\dot{\varepsilon}_2 \tag{46}$$

Then, using Eqs. (43) and (46), the following equation for the effective stain rate is obtained:

$$\dot{\bar{\varepsilon}} = b_1\left(1+\gamma\beta\right)\dot{\varepsilon}_1 \tag{47}$$

where b_1 is given in Eq. (19) or (20). From Eq. (18), we have:

$$\frac{\dot{\bar{\sigma}}}{\bar{\sigma}} = \frac{\dot{\sigma}_1}{\sigma_1} \tag{48}$$

Combining Eqs. (48), (47) and (40) gives:

$$\frac{\dot{\bar{\sigma}}}{\bar{\sigma}} = \frac{\dot{\bar{\varepsilon}}}{b_2} \tag{49}$$

where b_2 is:

$$b_2 = b_1\left(1+\gamma\beta\right) \tag{50}$$

Considering the constitutive equation as follows:

$$\bar{\sigma} = k\bar{\varepsilon}^n\dot{\bar{\varepsilon}}^m \tag{51}$$

Then, by applying the chain rule of differentiation to compute $\dot{\bar{\sigma}}$, we obtain:

$$\frac{\dot{\bar{\sigma}}}{\bar{\sigma}} = \frac{n}{\bar{\varepsilon}}\dot{\bar{\varepsilon}} + \frac{m}{\dot{\bar{\varepsilon}}}\ddot{\bar{\varepsilon}} \tag{52}$$

Equating the RHS of Eq. (52) and (49), $\ddot{\bar{\varepsilon}}$ is obtained as follows:

$$\ddot{\bar{\varepsilon}} = \left(\frac{\dot{\bar{\varepsilon}}}{b_2} - \frac{n\dot{\bar{\varepsilon}}}{\bar{\varepsilon}} \right) \frac{\dot{\bar{\varepsilon}}}{m} \tag{53}$$

Eq. (53) can be used as the governing differential equation phase II for the LHS of the FLD which is equivalent to that calculated by Pishbin and Gillis [18] for the LHS using case IV of Hill's non-quadratic flow law.

In the positive minor strain region (RHS) of the FLD, strain rate is assumed to remain uniform throughout the sheet. Therefore,

$$\dot{\varepsilon}_2 = \beta, \qquad \beta \geq 0 \tag{54}$$

Applying Eqs. (54) into Eq. (16) or (17) gives:
For case I:

$$\ddot{\bar{\varepsilon}} = \left[\begin{array}{l} \left(\frac{R+1}{2R+1-2^{M-1}R} \right)^{1/(M-1)} \left(\dot{\varepsilon}_1^{\,M/(M-1)} + \beta^{M/(M-1)} \right) + \\ \left(\frac{R+1}{2(2R+1)} \right)^{1/(M-1)} \left(1 - \left(\frac{2R+1}{2R+1-2^{M-1}R} \right)^{1/(M-1)} \right) \left(\dot{\varepsilon}_1 - \beta \right)^{M/(M-1)} \end{array} \right]^{(M-1)/M} \tag{55}$$

For case II:

$$\ddot{\bar{\varepsilon}} = \left(z_1 \left(\left| 2\dot{\varepsilon}_1 + \beta \right|^{M/(M-1)} + \left| 2\beta + \dot{\varepsilon}_1 \right|^{M/(M-1)} \right) + z_2 \left| \dot{\varepsilon}_1 + \beta \right|^{M/(M-1)} \right)^{(M-1)/M} \tag{56}$$

where,

$$z_1 = \left(\left(R+1 \right)(2^{M-1}-1) / \left(3^M + 2^{M-1} \left((R-1)(2^{M-1}-1) - 3 \right) \right) \right)^{1/M}$$

$$z_2 = \left((R+1)(2^{M-1}-1)/2 \right)^{1/(M-1)} - 2\left(3/2 \right)^{M/(M-1)} z_1$$

Eq. (55) or (56) can be solved explicitly for the effective strain rate in terms of strain rate and β or numerically for the strain rate when the effective strain rate and β are given.

Differentiating both sides of the Eq. (5) or (6), gives,
For case I:

$$\left(R+1 \right) \frac{\bar{\sigma}^{M-1}}{\sigma_1^{\,M-1}} \dot{\bar{\sigma}} = \left(2R+1 \right) \left(\dot{\sigma}_1 + \left(\frac{\sigma_2}{\sigma_1} \right)^{M-1} \dot{\sigma}_2 \right) - R \left(1 + \frac{\sigma_2}{\sigma_1} \right)^{M-1} \left(\dot{\sigma}_1 + \dot{\sigma}_2 \right) \tag{57}$$

For case II:

$$\begin{aligned} ((R+1)(2^{M-1}-1)-3) \frac{\bar{\sigma}^{M-1}}{\sigma_1^{\,M-1}} \dot{\bar{\sigma}} = & \left(2\frac{\sigma_2}{\sigma_1} - 1 \right)^{M-1} \left(2\dot{\sigma}_2 - \dot{\sigma}_1 \right) + \left(2 - \frac{\sigma_2}{\sigma_1} \right)^{M-1} \left(2\dot{\sigma}_1 - \dot{\sigma}_2 \right) \\ & + ((R-1)(2^{M-1}-1)-3) \left(1 - \frac{\sigma_2}{\sigma_1} \right)^{M-1} \left(\dot{\sigma}_1 - \dot{\sigma}_2 \right) \end{aligned} \tag{58}$$

Inserting Eq. (29) into Eq. (57) or (58) gives,
For case I:

$$(R+1)\left(\frac{\bar{\sigma}}{\sigma_1}\right)^M \frac{\dot{\bar{\sigma}}}{\bar{\sigma}} = \left(2R+1-R\left(1+\gamma\right)^{M-1}\right)\dot{\varepsilon}_1 + \left((2R+1)\gamma^M - R\gamma\left(1+\gamma\right)^{M-1}\right)\dot{\varepsilon}_2 \tag{59}$$

For case II:

$$((R+1)(2^{M-1}-1)-3)\left(\frac{\bar{\sigma}}{\sigma_1}\right)^M \frac{\dot{\bar{\sigma}}}{\bar{\sigma}} = \left(((R-1)(2^{M-1}-1)-3)\left(1-\gamma\right)^{M-1} - \left(2\gamma-1\right)^{M-1}\right)\dot{\varepsilon}_1 + \left(\gamma\left(2\gamma-1\right)^{M-1} - \gamma(((R-1)(2^{M-1}-1)-3)\left(1-\gamma\right)^{M-1}\right)\dot{\varepsilon}_2 \tag{60}$$

Rewriting Eq. (5) or (6), gives,
For case I:

$$(R+1)\left(\frac{\bar{\sigma}}{\sigma_1}\right)^M = (2R+1)(1+\gamma^M) - R(1+\gamma)^M \tag{61}$$

For case II:

$$((R+1)(2^{M-1}-1)-3)\left(\frac{\bar{\sigma}}{\sigma_1}\right)^M = \left(2-\gamma\right)^M + \left(2\gamma-1\right)^M + ((R-1)(2^{M-1}-1)-3)\left(1-\gamma\right)^M \tag{62}$$

Combining Eqs. (59), (61) and (54), the following equation is obtained,
For case I:

$$\frac{\dot{\bar{\sigma}}}{\bar{\sigma}} = \frac{\left(2R+1-R\left(1+\gamma\right)^{M-1}\right)\dot{\varepsilon}_1 + \left((2R+1)\gamma^M - R\gamma\left(1+\gamma\right)^{M-1}\right)\beta}{(2R+1)\left(1+\gamma^M\right) - R\left(1+\gamma\right)^M} \tag{63}$$

For case II:

$$\frac{\dot{\bar{\sigma}}}{\bar{\sigma}} = \frac{\left(((R-1)(2^{M-1}-1)-3)\left(1-\gamma\right)^{M-1} - \left(2\gamma-1\right)^{M-1}\right)\dot{\varepsilon}_1}{\left(2-\gamma\right)^M + \left(2\gamma-1\right)^M + ((R-1)(2^{M-1}-1)-3)\left(1-\gamma\right)^M} + \frac{\left(\gamma\left(2\gamma-1\right)^{M-1} - \gamma(((R-1)(2^{M-1}-1)-3)\left(1-\gamma\right)^{M-1}\right)\beta}{\left(2-\gamma\right)^M + \left(2\gamma-1\right)^M + ((R-1)(2^{M-1}-1)-3)\left(1-\gamma\right)^M} \tag{64}$$

Equating right hand side of Eqs. (52) and (63) and solving for $\ddot{\bar{\varepsilon}}$ gives:

$$\ddot{\bar{\varepsilon}} = \frac{W}{m}\dot{\bar{\varepsilon}} - \frac{n}{m}\frac{\dot{\bar{\varepsilon}}^2}{\bar{\varepsilon}} \tag{65}$$

where,
For case I:

$$W = \frac{\left((2R+1)\gamma^M - R\gamma\left(1+\gamma\right)^{M-1}\right)\beta + \left(2R+1-R\left(1+\gamma\right)^{M-1}\right)\dot{\varepsilon}_1}{(2R+1)\left(1+\gamma^M\right) - R\left(1+\gamma\right)^M} \tag{66}$$

For case II:

$$W=\frac{\left(((R-1)(2^{M-1}-1)-3)(1-\gamma)^{M-1}-(2\gamma-1)^{M-1}\right)\dot{\varepsilon}_1}{(2-\gamma)^M+(2\gamma-1)^M+((R-1)(2^{M-1}-1)-3)(1-\gamma)^M}+\frac{\left(\gamma(2\gamma-1)^{M-1}-\gamma((R-1)(2^{M-1}-1)-3)(1-\gamma)^{M-1}\right)\beta}{(2-\gamma)^M+(2\gamma-1)^M+((R-1)(2^{M-1}-1)-3)(1-\gamma)^M} \tag{67}$$

Eq. (66) or (67) can be taken as the governing differential equation during phase II for the RHS of the FLD. At each stage of the integration, $\dot{\varepsilon}_1$ is obtained from the effective strain rate using Eq. (55) or (56) and γ is obtained from Eq. (47).

2.2.3 Analysis of phase III

Localized necking is studied based upon the Bridgeman-type neck [32]. This neck is assumed to obey the kinematic constraint that is:

$$\frac{a}{r}=k\,Ln\left(\frac{h_0}{a}\right) \tag{68}$$

where *r* is the radius of curvature of the trace of the neck, 2a is the minimum thickness in the deforming sheet and *k* is a constant taken here as ¾.

The thinning rate $\dot{\varepsilon}_n$ at the minimum cross-section is found by considering deformation rate for the 1 direction of the sheet. The material velocity component normal to the neck is considered to accommodate the prescribed deformation program in the 1 direction by the strain only within the skewed neck. Hill's velocity discontinuity analysis is used to determine the necessary formulation [9]. The thinning rate in the minimum cross-section during phase III is, for the LHS,

$$\dot{\varepsilon}_n=\frac{(1+\beta)(L_0/2h_0)(\dot{L}/L_0)\cos(\theta)k\varepsilon_n^2\exp(\varepsilon_n)}{F(\varepsilon_n)} \tag{69}$$

For the RHS,

$$\dot{\varepsilon}_n=\frac{(L_0/2h_0)(\dot{L}/L_0)k\varepsilon_n^2\exp(\varepsilon_n)+\varepsilon_n\dot{\varepsilon}_2\sin(\varphi)}{F(\varepsilon_n)} \tag{70}$$

where,

$$F(\varepsilon_n)=2\left[\left(1+2\varepsilon_n+k\varepsilon_n^2\right)/\left(1+2/k\varepsilon_n\right)\right]^{1/2}\times\arctan\left[\varepsilon_n\left(2+k\varepsilon_n\right)/\left(2+2\varepsilon_n+k\varepsilon_n^2\right)\right]^{1/2}-\left(1+\varepsilon_n+k\varepsilon_n^2\right)\Phi \tag{71}$$

where φ is given by:

$$\cos(\Phi)=(1+\varepsilon_n)/\left(1+\varepsilon_n+k\varepsilon_n^2\right) \tag{72}$$

The specific procedure for deriving the equations above has been given by Pishbin and Gillis [18]. The neck strain ε_n, can be related to conditions in phase II as following:

$$\varepsilon_{\mathrm{n}}=\varepsilon_3(\mathrm{II})+Ln\left[\frac{\left(1+2\varepsilon_n+k\varepsilon_n^2\right)}{\left(1+\varepsilon_n+k\varepsilon_n^2\right)}\right] \tag{73}$$

Eq. (73) can be solved numerically. Once the value of ε_n is obtained from Eq. (73), it is substituted into Eq. (69) to calculate the thinning rate. After determining the thinning rate in the minimum cross-section, the strain rate is easily obtained as:

$$\dot{\varepsilon}_1(\mathrm{III}) = \dot{\varepsilon}_n/(1+\rho) \qquad \text{For the LHS of the FLD} \tag{74}$$

$$\dot{\varepsilon}_1(\mathrm{III}) = \dot{\varepsilon}_n - \dot{\varepsilon}_2 \qquad \text{For the RHS of the FLD} \tag{75}$$

2.2.4 Calculation of forming limit strains

It is interesting to note that actual limit strains are mainly measured at some distance away from the failure. Here, it is assumed that the minor strain at point *J*, remains constant. For the LHS of the FLD, proportional straining is assumed so that $e_2/e_1 = \rho$. From the conservation of volume at the center of the neck at time *J*,

$$\varepsilon_1^J = \varepsilon_n/(1+\rho) \tag{76}$$

$$\varepsilon_2^J = \rho\varepsilon_n/(1+\rho) \tag{77}$$

Now from the constancy of volume, the limit strains are

$$\varepsilon_1^* = -\varepsilon_2^J - \varepsilon_3(\mathrm{II}) \tag{78}$$

$$\varepsilon_2^* = \varepsilon_2^J \tag{79}$$

where ,

$$\varepsilon_3(\mathrm{II}) = -\varepsilon_n + Ln\left(1 + \frac{1-\cos\Phi}{k\varepsilon_n}\right) \tag{80}$$

For the RHS of the FLD, ε_2 is assumed to be homogenous. At time *J*, $\varepsilon_2(\mathrm{II}) = \varepsilon_2(\mathrm{III})$ thus,

$$\varepsilon_1^J = \varepsilon_n - \varepsilon_2(\mathrm{II}) \tag{81}$$

$$\varepsilon_2^J = \varepsilon_2(\mathrm{II}) \tag{82}$$

The values of the limit strains obtained from Eqs. (78) and (79) are transformed to engineering strain values to plot the FLD.

$$e_1 = \exp(\varepsilon_1^*) - 1 \tag{83}$$

$$e_2 = \exp(\varepsilon_2^*) - 1 \tag{84}$$

2.3 M-K model

Analysis of the neck in M-K model is based upon that the groove is normal to the principle stress. The strain increment inside the groove ($d\varepsilon_{b1}$) is considered and the corresponding strain in the safe zone ($d\varepsilon_{a1}$) is calculated

based on an iterative procedure. The procedure consisted of applying an increment of $d\varepsilon_{b1}$ and then guessing $\Delta\varepsilon_{a1}$. $d\varepsilon_{a2}$ can be obtained as $d\varepsilon_{a2}=\rho_a\Delta\varepsilon_{al}$. Concerning compatibility condition, $d\varepsilon_{a2}=d\varepsilon_{b2}$, we have:

$$\rho_b=\frac{d\varepsilon_{b2}}{d\varepsilon_{b1}} \tag{85}$$

$$\Delta\varepsilon_{a3}=-\left(1+\rho_a\right)\Delta\varepsilon_{a1} \tag{86}$$

$$\Delta\varepsilon_{b3}=-\left(1+\rho_b\right)d\varepsilon_{b1} \tag{87}$$

Considering the strain increment, the effective stress-strain equation, Eq. (51), is modified as following:

$$\bar{\sigma}=k\left(\bar{\varepsilon}+\Delta\bar{\varepsilon}\right)^n\dot{\bar{\varepsilon}}^m \tag{88}$$

The force equilibrium results in:

$$F_{1a}=F_{1b} \tag{89}$$

$$\sigma_{1a}t_a=\sigma_{1b}t_b \tag{90}$$

where F_1 and σ_1 are the force and the stress normal to the groove. For natural strain we have:

$$\sigma_{1a}t_{0a}\exp(\varepsilon_{a3})=\sigma_{1b}t_{0b}\exp(\varepsilon_{b3}) \tag{91}$$

Inserting Eq. (88) in Eq. (91):

$$\psi_a\left(\bar{\varepsilon}_a+d\bar{\varepsilon}_a\right)^n=\psi_b f_0\exp(\varepsilon_{b3}-\varepsilon_{a3})\left(\bar{\varepsilon}_b+d\bar{\varepsilon}_b\right)^n\left(\frac{\beta_b\rho_a}{\beta_a\rho_b}\right)^m \tag{92}$$

where,

$$\beta=\frac{\Delta\bar{\varepsilon}}{\Delta\varepsilon_1}=\psi\left(1+\gamma\rho\right)\ \ and\ \ \psi=\sigma_1/\sigma_2 \tag{93}$$

The value of ψ can be calculated for case I and case II of Hill's non-quadratic flow law according to Eqs. (19) and (20), respectively.

Using associated flow rules for plastic deformation, $d\varepsilon_i=\frac{\partial\bar{\sigma}}{\partial\sigma_i}d\lambda$, the strain ratio can be obtained as:

Case I:

$$\rho=\frac{\left(2R+1\right)\gamma^{M-1}-R\left(1+\gamma\right)^{M-1}}{\left(2R+1\right)-R\left(1+\gamma\right)^{M-1}} \tag{94}$$

Case II:

$$\rho = \frac{2(2\gamma-1)^{M-1} - (2-\gamma)^{M-1} - \left((R-1)(2^{M-1}-1)-3\right)(1-\gamma)^{M-1}}{2(2-\gamma)^{M-1} - (2\gamma-1)^{M-1} + \left((R-1)(2^{M-1}-1)-3\right)(1-\gamma)^{M-1}} \tag{95}$$

The procedure to calculate limit strains is as following. (i) Using Eq. (92) and Eq. (93) to calculate $d\bar{\varepsilon}_a$ and $d\varepsilon_{al}$, respectively. (ii) Strain increment $d\varepsilon_{bl}$ is applied until $d\varepsilon_{b1} > 10\, d\varepsilon_{a1}$. (iii) The corresponding $\varepsilon_{a1}, \varepsilon_{a2}$ is used to plot the FLD.

3 RESULTS AND DISCUSSION

In order to assess the validity of the present analysis, comparisons were made with experimental FLDs. All the material constants needed for the calculation of FLDs, are taken from other references [14,18,33,34]. In calculation of FLDs, average of weighted values of mechanical properties, such as *n* and *r* are defined as $t = (t_0 + 2t_{45} + t_{90})/4$. In case I and case II of Hill's 1979 nonquadratic flow law, which is used in this analysis, the exponent *M* is greater than one and must be determined experimentally. In the present wok, this exponent is used as an adjustable parameter to obtain a best fit between the calculated and experimental FLDs.

3.1 Comparison with experiment

Calculated FLDs were compared with experimental FLDs of three materials reported by other references. The capability of the model to predict experimental results was investigated. All material constants used in calculations are given in Table 1.

Fig. 3 shows predicted and experimental FLDs for AK steel reported by other references. In both LHS and RHS of the FLD the agreement is fair for the J-G model. But, in the LHS of the FLD calculations show better agreement for the M-K model.

Fig. 4 shows the calculated and experimental FLDs for aluminum 2036-T4 reported by other references. The agreement between experimental and calculated results is acceptable for J-G model. However, agreement between M-K predictions and experiments are poor. Fig. 5 compares calculated FLDs with experimental ones for aluminum 3003-O. The correlation between experimental and calculated FLDs is very good for J-G model. It should be noted that predicted limit strains in case I are smaller than case II in the positive strain region. However, the LHS of calculated FLDs are identical. M-K predictions are poor for both case I and case II.

Table 1
Mechanical properties of studied materials.

Material	Angle to the rolling direction (deg.)	Strain rate sensitivity index (m)	Strain hardening exponent (n)	Plastic strain ratio (R)
2036-T4 aluminum	0	-	-	0.68
	45	0.13[a]	0.005[b]	0.65[a]
	90	–	-	1.13
3003-O aluminum	0	–	0.190	1.08
	45	0.005[c]	0.200[d]	0.85[d]
	90	–	0.193	0.25
AK steel	0	-	-	1.70
	45	0.012[c]	0.228[c]	1.27[c]
	90	-	-	2.13

[a]Ref. 18
[b]Ref.27
[c]Ref.14
[d]Ref. 28

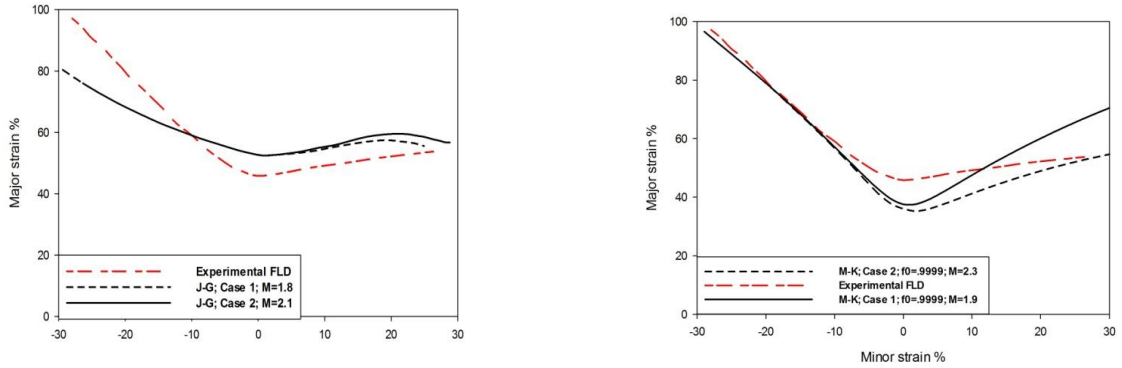

Fig.3
Experimental and predicted FLDs for AK steel, experimental data are from [14].

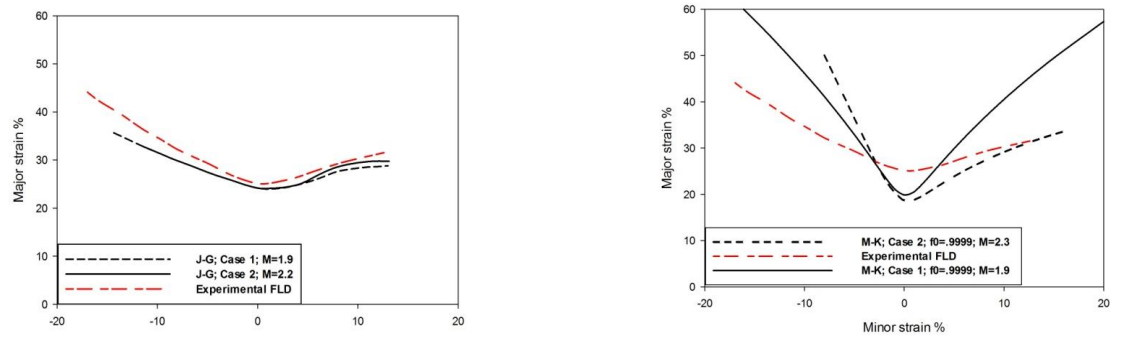

Fig.4
Experimental and predicted FLDs for aluminum 2036-T4, experimental data are from [18, 27].

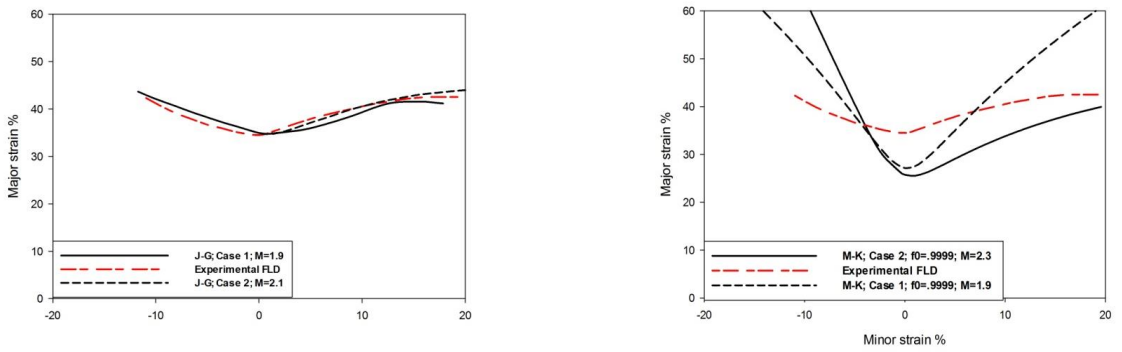

Fig.5
Experimental and predicted FLDs for aluminum 3003-O, experimental data are from [14, 28].

3.2 Influence of material parameters

In order to check the influence of material properties on the limit strain, the computation was done for AK steel as a representative material. Fig. 6 shows the effect of the strain rate sensitivity parameter (m) on calculated FLDs for the AK steel. Based on the case I of Hill's yield criterion, increasing the value of m results in raising the level of both sides of the FLD. This is in agreement with the experimental observations, indicating that uniform strain distribution is achieved by higher strain rate sensitivity index.

The effect of the strain hardening exponent (n) on the FLD is demonstrated in Fig. 7. Increasing the n value shifts the FLD to higher values. Fig. 8 shows the influence of the plastic anisotropy ratio on the calculated FLD. In the RHS of the FLD, with increasing R values, forming limit strains attain higher level. However, in the LHS of the FLD, changing R did not affect the level of the FLD.

Fig. 9 shows the effect of exponent *M* on the predicted FLD. An increase in *M* results in an increase in the limit strains for the positive strain region, while it has no effect on the limit strains in the negative minor strain and the plane strain regions of the FLD.

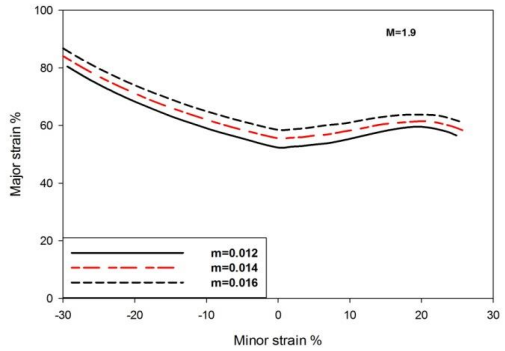

Fig.6
Influence of strain rate sensitivity (m) on the calculated FLD for AK steel.

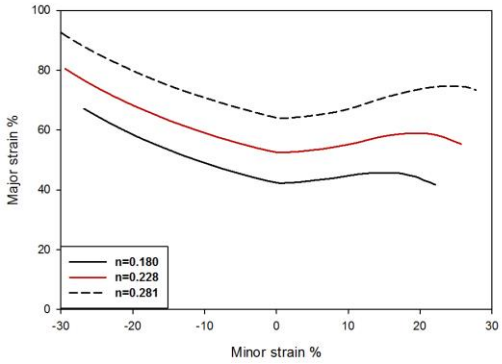

Fig.7
Influence of strain hardening exponent (n) on the calculated FLD for AK steel.

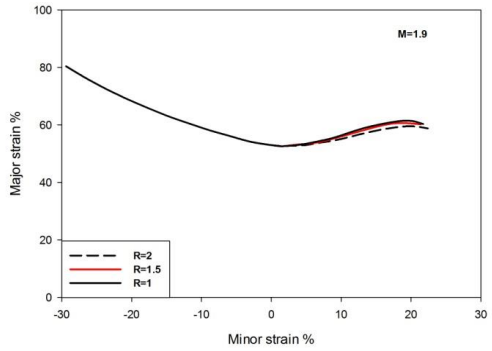

Fig.8
Influence of plastic anisotropy ratio on the calculated FLD for AK steel.

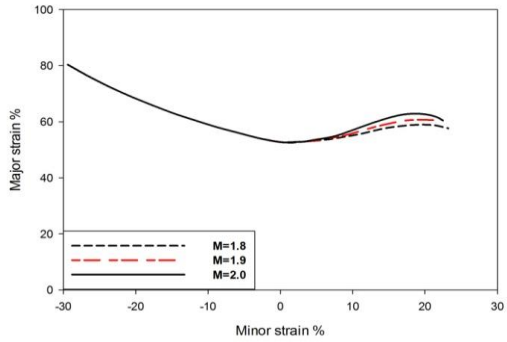

Fig.9
Influence of the Hill's exponent on the calculated FLD for AK steel.

3.3 Comparison to the Hill's 1993 criterion

The general form of the criterion proposed by Hill in 1993 [35] is:

$$\frac{\sigma_1^{\,2}}{\sigma_0^{\,2}}-\frac{c\sigma_1\sigma_2}{\sigma_0\sigma_{90}}+\frac{\sigma_2^2}{\sigma_{90}^2}+\left\{\left(p+q\right)-\frac{p\sigma_1+q\sigma_2}{\sigma_b}\right\}\frac{\sigma_1\sigma_2}{\sigma_0\sigma_{90}}=1$$

where c, p and q are non-dimensional parameters and given by:

$$\frac{c}{\sigma_0\sigma_{90}}=\frac{1}{\sigma_0^2}+\frac{1}{\sigma_{90}^2}-\frac{1}{\sigma_b^2}$$

$$\left(\frac{1}{\sigma_0}+\frac{1}{\sigma_{90}}-\frac{1}{\sigma_b}\right)p=\frac{2r_0\left(\sigma_b-\sigma_{90}\right)}{\left(1+r_0\right)\sigma_0^2}-\frac{2r_{90}\sigma_b}{\left(1+r_{90}\right)\sigma_{90}^2}+\frac{c}{\sigma_0}$$

$$\left(\frac{1}{\sigma_0}+\frac{1}{\sigma_{90}}-\frac{1}{\sigma_b}\right)q=\frac{2r_0\left(\sigma_b-\sigma_0\right)}{\left(1+r_{90}\right)\sigma_{90}^2}-\frac{2r_0\sigma_b}{\left(1+r_{90}\right)\sigma_0^2}+\frac{c}{\sigma_{90}}$$

In the above equations, σ_b is the yield stress under balanced biaxial tension, σ_0 and σ_{90} are yield stresses under uniaxial tension at 0° and 90° to the rolling direction, respectively, and r_0 and r_{90} are ratios of transverse to through-thickness increments of logarithmic strain under σ_0 and σ_{90}, respectively. It is noted that there are five independent material parameters σ_0, σ_{90}, σ_b, r_0, and r_{90} among which no presumed relationship is postulated. These parameters need to be determined for each material experimentally. The J-G model based on the Hill's 1993 criterion has been discussed by Rezaee-Bazzaz et al [22]. The reported result for AA3003 can be compared to the present analysis. The results of comparison are as following.

Hill's 1993 criterion overestimates FLD_0 and the LHS of the AA3003 FLD. However, case I and II results in the presented analysis are much closer to the experiment. Considering the RHS of the FLD, the Hill's 1993 criterion prediction is a bit greater than the experiment. In contrast, case I and II results are smaller than the experiment and are more accurate than Hill's 1993 criterion. Moreover, Hill's 1993 criterion has the capability of calculating larger strains than that of case I and II criteria.

The above mentioned differences between Hill's 1979 and 1993 yield criteria can be discussed based on different terms and coefficients used in yield functions. For instance, the LHS of the FLD based on Hill's 1993 is calculated according to the following equation [22]:

$$\ddot{\varepsilon}_1=\left(1-\frac{n}{\varepsilon_1}\right)\frac{\dot{\varepsilon}_1^2}{m}$$

However, for Hill's 1979 the LHS is calculated based on the Eqs. (55) and (56). It is clear that for Hill's1993 the limit strain depends on experimental parameters n and m. Considering Hill's 1979, the limit strain depends on anisotropy parameter R and M.

Hill's 1993 yield criterion is based on experimental values that should be precisely derived. In contrast, Hill's 1979 is mainly based on M parameter that is an adjustable parameter and usually takes a proper value to fit the experimental data. Consequently, it is expected that Hill's1979 results would be closer to the experiment especially when experimental coefficients of Hill's 1993 were inaccurately calculated. Moreover, adjustable exponent M in Hill's 1979 leads to much nonlinearity of equations when it is compared to the quadratic Hill's 1993 yield function. Consequently, much solution errors are expected in the case of Hill's 1979 yield function. However, it should be noted that these errors may be insignificant when precise numerical methods and powerful software are used.

Increasing R value results in greater strains in the RHS when Hill's 1993 criterion is used. However, this is vise versa for case I and II criteria. Increasing m, n and M parameters result in shifting the FLD to the higher levels in both Hill's 1993 and case I and II criteria. RHS of the FLD for Hill's 1979 is calculated based on Eq. (65) that is directly dependent on $W.W$ is related to R According to Eq. (66) and decreased with increasing of R. However, LHS of the FLD for Hill's 1993 has no direct relation to R value based on Rezaee-Bazzaz et al [22] derivations.

4 CONCLUSIONS

Case I and case II of Hill's non-quadratic yield function were used to predict forming limit strains based on both J-G and M-K models. The following conclusions can be drawn from the analysis.

1. J-G predictions for FLDs are in better agreement with experiments than M-K model when case I or case II of Hill's non-quadratic yield function is used.
2. Considering yield function exponent (M), the best agreement to experiments achieved when M<2 for case I and M>2 for case II. Increasing M or normal anisotropy (R) affects the RHS of FLD and has no effect on the LHS.
3. Limit strain predictions for case I of Hill's non-quadratic yield function in the RHS of the FLD are greater than case II predictions for M-K model. However, there is no significant difference when J-G model is used.
4. Considering LHS and RHS of the FLD, Predictions based on the case I and II criteria for AA3003 are closer to the experiment than the predictions of the Hill's 1993 criterion.

REFERENCES

[1] Keeler S.P., 1969, Circular grid system: a valuable aid for evaluation sheet forming, *Sheet Metal Industrial* **45**: 633-640.

[2] Goodwin G.M., 1969, Application of strain analysis to sheet metal forming problems, *Metall Ital* **60**: 767-771.

[3] Liu J., Liu W., Xue W., 2013, Forming limit diagram prediction of 5052/polyethylene/AA5052 sandwich sheets, *Materials and Design* **46**: 112-120.

[4] Aghaie-Khafri M., Mahmudi R., 2005, The effect of preheating on the formability of an Al–Fe–Si alloy sheet, *Journal of Materials Processing Technology* **169**: 38-43.

[5] Friedman P.A., Pan J., 2000, Effects of plastic anisotropy and yield criteria on prediction of forming limit curves, *International Journal of Mechanical Sciences* **42**: 29-48.

[6] Zhang L., Wang J., 2012, Modeling the localized necking in anisotropic sheet metals, *International Journal of Plasticity* **39**: 103-118**.**

[7] Velmanirajan K., Syed Abu Thaheer A., Narayanasamy R., Ahamed Basha C., 2012, Numerical modelling of aluminium sheets formability using response surface methodology, *Materials and Design* **41**: 239-254.

[8] Hart E.W., 1967, Theory of the tensile test, *Acta Metallurgica* **15**: 351-355.

[9] Hill R., 1952, On discontinuous plastic states with special reference to localized necking in thin sheets, *Journal of the Mechanics and Physics of Solids* **1**: 19-30.

[10] Gillis P.P., Jones S.E., 1979, Tensile deformation of a flat sheet, *International Journal of Mechanical Sciences* **21**: 109-117.

[11] Marciniak Z., Kuczynski K., 1967, Limit strains in the processes of stretch-forming sheet metal, *International Journal of Mechanical Sciences* **9**: 609-620.

[12] Mohebbi M.S., Akbarzadeh A., 2012, Prediction of formability of tailor welded blanks by modification of MK model, *International Journal of Mechanical Sciences* **61**: 44-51.

[13] Jones S.E., Gillis P.P., 1984, An analysis of biaxial stretching of a flat sheet, *Metallurgical Transactions A* **15**: 133-138.

[14] Choi W., Gillis P.P., Jones S.E ., 1989, Calculation of the forming limit diagram, *Metallurgical Transactions A* **20**:1975-1987.

[15] Choi W., Gillis P.P., Jones S.E., 1989, *Forming Limit Diagrams: Concepts, Methods and Applications*, edited by Wagoner R.H., Chan K.S., Keeler S.P., Published, TMS Warendale.

[16] Jones S.E., Gillis P.P., 1984, Analysis of biaxial stretching of a flat sheet, *Metallurgical Transactions A* **15**: 133-138.

[17] Jones S.E., Gillis P.P., 1984, Generalized quadratic flow law for sheet metals, *Metallurgical Transactions A* **15**: 129-132.

[18] Pishbin H., Gillis P.P., 1992, Forming limit diagrams calculated using Hill's nonquadratic yield criterion, *Metallurgical Transactions A* **23**: 2817-2831.

[19] Aghaie-Khafri M., Mahmudi R., 2004, Predicting of plastic instability and forming limit diagrams, *International Journal of Mechanical Sciences* **46**: 1289-1306.

[20] Aghaie-Khafri M., Mahmudi R., Pishbin H., 2002, Role of yield criteria and hardening laws in the prediction of forming limit diagrams, *Metallurgical Transactions A* **33**: 1363-1371.

[21] Noori H., Mahmudi R., 2007, Prediction of forming limit diagrams in sheet metals using different yield criteria, *Metallurgical Transactions A* **38**: 2040-2052.

[22] Rezaee-Bazzaz A., Noori H., Mahmudi R., 2011, Calculation of forming limit diagrams using Hill's 1993 yield criterion, *International Journal of Mechanical Sciences* **53**: 262-270.

[23] Chung K., Kim H., Lee C., 2014, Forming limit criterion for ductile anisotropic sheets as a material property and its deformation path insensitivity. Part I: Deformation path insensitive formula based on theoretical models, *International Journal of Plasticity* **58**: 3-34.
[24] Avila A.F., Vieira E.L.S., 2003, Proposing a better forming limit diagram prediction: a comparative study, *Journal of Materials Processing Technology* **141**: 101-108.
[25] Chiba R., Takeuchi H., Kuroda M., Kuwabara T., 2013, Theoretical and experimental study of forming-limit strain of half-hard AA1100 aluminium alloy, *Computational Materials Science* **77**: 61-71.
[26] Panich S., Barlat F., Uthaisangsuk V., Suranuntchai S., Jirathearanat S., 2013, Experimental and theoretical formability analysis using strain and stress based forming limit diagram for advanced high strength steels, *Materials & Design* **51** : 756-766.
[27] Assempour A., Hashemi R., Abrinia K., Ganjiani M., Masoumi E., 2009, A methodology for prediction of forming limit stress diagrams considering the strain path effect, *Computational Materials Science* **45**: 195-204.
[28] Kuroda M., Tvergaard V., 2000, Forming limit diagrams for anisotropic metal sheets with different yield criteria, *International Journal of Solids and Structures* **37**: 5037-5059.
[29] Hill R., 1979, Theoretical plasticity of textured aggregates, *Mathematical Proceedings of the Cambridge Philosophical Society* **75**: 179-191.
[30] Lian J., Zhou D., Baudelet B., 1989, Application of Hill's new yield theory to sheet metal forming part I. Hill's 1979 criterion and its application to predicting sheet forming limit, *International Journal of Mechanical Sciences* **31**: 237-247.
[31] Considére A., 1885, *Annales des Ponts et Chaussées* **9**: 574-775.
[32] Bridgeman P.W., 1952, *Studies in Large Plastic Flow and Fracture*, McGraw-Hill, New York.
[33] Ghosh A.K., 1977, The Influence of Strain Hardening and Strain-Rate Sensitivity on Sheet Metal Forming, Trans ASME: *Journal of Engineering Materials and Technology* **99**: 264-274.
[34] Hecker S.S., 1975, Formability of aluminum alloy sheets, Trans ASME: *Journal of Engineering Materials and Technology* **97**: 66-73.
[35] Hill R., 1993, A user-friendly theory of orthotropic plasticity in sheet metals, *International Journal of Mechanical Sciences* **35**:19-25.